Variation in bulk-leaf ^{13}C discrimination, leaf traits and water-use efficiency-trait relationships along a continental-scale climate gradient in Australia

Running head: WUE_i and trait relationships across Australia

Rizwana Rumman[1], Owen K Atkin[2], Keith J Bloomfield[3] and Derek Eamus[1,4]

[1]Terrestrial Ecohydrology Research Group
School of Life Sciences
University of Technology Sydney
PO Box 123
NSW 2007
Australia

[2] ARC Centre of Excellence in Plant Energy Biology, Research School of Biology, Building 134, The Australian National University, Canberra, ACT 2601, Australia.

[3] Division of Plant Sciences, Research School of Biology, Building 46, The Australian National University, Canberra, ACT 2601, Australia

[4] Corresponding author: +61 2 9514 4154; Derek.Eamus@uts.edu.au

Key words: ^{13}C, isotope discrimination, leaf traits, climate and WUE_i

Abstract

Large spatial and temporal gradients in rainfall and temperature occur across Australia. This heterogeneity drives ecological differentiation in vegetation structure and ecophysiology. We examined multiple leaf-scale traits, including foliar ^{13}C isotope discrimination (Δ^{13}C), rates of photosynthesis and foliar N concentration and their relationships with multiple climate variables. 55 species across 27 families were examined across eight sites spanning contrasting biomes.

Key questions addressed include: 1) Does Δ^{13}C and intrinsic water use efficiency (WUE$_i$) vary with climate at a continental scale? 2) What are the seasonal and spatial patterns in Δ^{13}C / WUE$_i$ across biomes and species? 3) To what extent does Δ^{13}C reflect variation in leaf structural, functional and nutrient traits across climate gradients? and 4) Does the relative importance of assimilation and stomatal conductance in driving variation in Δ^{13}C differ across seasons?

We found that MAP, temperature seasonality, isothermality and annual temperature range exerted independent effects on foliar Δ^{13}C / WUE$_i$. Temperature-related variables exerted larger effects than rainfall-related variables. The relative importance of photosynthesis and stomatal conductance (g_s) in determining Δ^{13}C differed across seasons: Δ^{13}C was more strongly regulated by g_s during the dry season and by photosynthetic capacity during the wet-season.

Δ^{13}C was most strongly correlated, inversely, with leaf mass area ratio among all leaf attributes considered.

Leaf N$_{mass}$ was significantly and positively correlated with MAP during dry- and wet- seasons and with moisture index (MI) during the wet-season but was not correlated with Δ^{13}C. Leaf P$_{mass}$ showed significant positive relationship with MAP and Δ^{13}C only during the dry-season. For all leaf nutrient-related traits, the relationships obtained for Δ^{13}C with MAP or MI indicated that Δ^{13}C at the species level reliably reflects the water status at the site level. Temperature and water availability, not foliar nutrient content, are the principal factors influencing Δ^{13}C across Australia.

Introduction

Vegetation structure and function is strongly modulated by climate. Consequently, understanding plant physiological responses to climate gradients is critical for understanding spatial variation in ecosystem processes (Koch *et al.*, 1995, Schulze *et al.*, 1996) and their responses to climate variability. In Australia climate gradients are dominated by differences in the amount and timing of rainfall and average summer and winter temperatures. Collectively these determine the key differences among climate zones (Eamus *et al.*, 2006). Mean annual precipitation ranges from very low (< 250 mm) in Central Australia to high (> 4000 mm) in NE Australia. Mean maximum temperatures increase with decreasing latitude and distance from the coast. Spatial and temporal heterogeneity in temperature and rainfall has been demonstrated to strongly influence physiological and structural trait values, including foliar nitrogen content, specific leaf area, photosynthetic capacity and water-use-efficiencies (e.g. Cernusak *et al.,* 2013, Wright *et al.,* 2004, Zhuang et al., 2016) along spatial gradients of environmental variables and also in response to seasonal variation is these variables (Eamus *et al.,* 2016).

Functional and structural attributes of vegetation often change in a predictable manner along gradients of water availability. For example, across sites with varying depth-to-groundwater, aboveground biomass and net primary productivity increased and water-use-efficiency decreased as water availability increased (Zolfaghar *et al.*, 2014). Water availability significantly influences rates of sap flow and annual rates of water use of trees (Dragoni *et al.*, 2009, Rossatto *et al.*, 2012, Whitley *et al.*, 2013, Zeppel *et al.*, 2008). Trees adapted to low rainfall exhibit a suite of traits, including the tendency to have sclerophyllous leaves (Eamus *et al.*, 2006, Fonseca *et al.*, 2000, Turner, 1994), large foliar concentrations of nitrogen and large wood densities (Cunningham *et al.*, 1999, Schulze *et al.*, 1998, Taylor & Eamus, 2008, Wright *et al.*, 2001). In this paper we examine numerous tree species across nine sites differing in mean annual precipitation and temperature, and seasonality of precipitation and temperature, to examine the response of multiple physiological and structural trait values to this variation.

The worldwide leaf economics spectrum highlights the importance of quantifying relationships among leaf traits (e.g. leaf mass per unit area, leaf life-span), how these traits differ between plant functional types and how differences in climate influence trait values and relationships among traits (Wright *et al*., 2005, Moles *et al.,* 2014). These relationships are gaining increased application in ecosystem models (Wright *et al.*, 2004, Lu *et al.*, 2017, Verheijen *et al.*, 2013), because many leaf-scale attributes scale strongly with several whole-plant properties (e.g. relative growth rate) and ecosystem properties (e.g. net primary productivity; Lambers & Poorter, 1992, Reich *et al.*, 1992). Globally, temperatures (range and mean values) and precipitation (timing and amount) are changing and are predicted to continue to change during the 21st century (CSIRO and Bureau of Meteorology 2015). Understanding current relationships among climate attributes and leaf physiological and structural traits at large-scales are central to the refinement of dynamic global vegetation models (Verheijen *et al*., 2013) for realistic assessments of future trajectories of plant behaviour as climate changes at regional scales. Analyses of these large-scale relationships contribute to assessments of fundamental ecological questions pertaining to plant ecological strategies, explanations of observed distribution of different plant communities (Moles *et al.,* 2014), and responses to future climate change.

Water-use-efficiency (WUE) and intrinsic water-use-efficiency (WUE_i) are responsive to abiotic and biotic factors, including photosynthetic potential, rainfall and vapour pressure deficit (Eamus *et al.,* 2016). Analyses of foliar $\delta^{13}C$ (isotopic signature; the ratio of ^{13}C to ^{12}C in leaves) can identify leaf gas exchange characteristics in C3 terrestrial plants within and across communities (Cernusak *et al.*, 2013, Diefendorf *et al.*, 2010, Kohn, 2010) and provides a good proxy of leaf-scale WUE_i (the ratio of net photosynthetic rate to stomatal conductance; Farquhar *et al.*, 1989, Farquhar, 1991, , Livingston & Spittlehouse, 1996) . More importantly, WUE_i is an integrated measure of the relative efficiency of carbon gain through photosynthesis, in terms of water transpired. Both C gain and transpiration are modulated by multiple abiotic and biotic factors. Future changes in climate will alter regional patterns in rainfall and temperature coincident with changes in atmospheric CO_2 concentration, all of which influence carbon and water fluxes through multiple interactions. Our understanding of the relative importance of different factors in determining WUE_i remains scant. Whilst there has been a focus on the effects of atmospheric CO_2 concentration on stomatal conductance and photosynthesis (Ainsworth & Rogers, 2007, Medlyn *et al.*, 2011), more detailed analyses of the impact of additional variables on WUE_i are required. We address this knowledge gap at a continental-scale.

Responses of foliar isotope discrimination ($\Delta^{13}C$, as opposed to $\delta^{13}C$, foliar isotopic signature; the ratio of ^{13}C to ^{12}C in leaves) to mean annual precipitation (MAP) have been examined in two recent global meta-analyses (Diefendorf *et al.*, 2010, Kohn, 2010). Diefendorf *et al.*, (2010) combined 3,310 published leaf $\Delta^{13}C$ values for 334 woody plant species at 105 locations; however, these data did not include Australian species, which are phylogenetically distinct from trees from most other parts of the world. The Kohn (2010) global-study encompassed multiple plant functional types and species from approximately 570 sites. Both studies reported decreasing $\Delta^{13}C$ with decreasing MAP, and MAP explained about half of the variation in $\Delta^{13}C$ globally. Similarly, Stewart et al., (1995) examined variation in $\delta^{13}C$ in 12 plant communities along a rainfall gradient in southern Queensland and found a strong response of mean $\delta^{13}C$ to MAP. By contrast, several studies in northern Australia (Cernusak *et al.*, 2011, Miller *et al.*, 2001, Schulze *et al.*, 1998) and in south-western Australia (Schulze *et al.*, 2006, Turner *et al.*, 2008) observed only weak community-level responses of $\delta^{13}C$ to MAP.

In contrast to the majority of Australian studies, which investigated closely related species within the genus *Eucalyptus,* the present study examined how $\Delta^{13}C$ (discrimination) responds to variation in climate from 37 genera sampled across continental Australia in tropical, temperate, arid and mesic sites. We also examine relationships among multiple leaf traits, multiple climate variables and WUE_i of 56 dominant tree to provide an understanding of patterns in climate-leaf traits-WUE_i interactions.

The objectives of our study were to address the following hypotheses:

1) Foliar discrimination against ^{13}C (and hence WUE_i) is more strongly affected by differences in precipitation than temperature.
2) Seasonality of precipitation has a larger impact on foliar discrimination against ^{13}C than seasonality in temperature.
3) Differences in precipitation are more important that differences in foliar N or P in explaining differences in foliar discrimination against ^{13}C.
4) The relative contribution of changes in photosynthetic capacity was larger than that of the contribution of changes in stomatal conductance to variation in $\Delta^{13}C$ in the wet-season but not the dry-season.

Materials and methods

Study area

The study accessed eight nodes of the Australian SuperSite Network across the continent. This Network (http://www.tern-supersites.net.au/) is a part of the Terrestrial Ecosystem Research Network (TERN), a federally funded initiative of the Australian government. Each SuperSite is a distinctly different type of ecosystem. Multiple data streams collected from these SuperSites provide a novel opportunity to combine and compare contrasting ecosystems across continental Australia.

The location, mean annual precipitation and mean annual temperature for each of the eight sites are given in Table 1. A map of the locations is given in Supplementary Material and the location of each site within the Whittaker Biome diagram is also given therein.

Site descriptions

These eight sites represent seven biomes with mean annual temperature (MAT) ranging from 10°C to ~28°C and mean annual precipitation (MAP) from 255 to 5,700 mm per year. A brief description of each site is given in Supplementary Material.

Study species

Each site is comprised of a one hectare plot within the footprint of the eddy covariance flux tower located at each SuperSite. Within each hectare, replicated measurements were made on dominant and mostly broadleaf evergreen overstorey species that collectively accounted for *ca* 80% of the (aboveground) biomass of each site. Across all sites a total of 55 plant species were sampled in the dry-season and 44 species sampled in the wet-season (417 individual trees from 27 plant families). Identical measurements were made of foliar $\delta^{13}C$ on four to six selected individuals of each species, from which $\Delta^{13}C$ was calculated. Variation in 16 additional leaf attributes (gas-exchange characteristics, structural and nutrient traits, see Table 2 for details) across the SuperSites and their relationships with $\Delta^{13}C$ were also examined.

Environmental variables

To quantify the climatic conditions for each of the eight nodes, 19 variables were used (11 temperature related and eight precipitation related parameters; Supplementary Material Table 2). Long term average data were obtained from the WorldClim database http://www.worldclim.org/, (Hijmans *et al.*, 2005) with a spatial resolution of 1 km, except for Cape Tribulation where OzFLux site average data were used for precipitation related parameters.

Leaf-trait data

Leaf gas exchange and additional leaf-traits (Table 2) were measured on 407 individual plants across 80 species at each of the seven Supersites (Table 1), generally across winter and summer seasons or wet- and dry-seasons. Leaf gas exchange was measured in the morning using a portable photosynthesis system (Li-Cor 6400; Li-Cor, Nebraska, USA) on upper canopy, fully expanded leaves on detached branches. Where there was evidence of an impact of detachment on gas exchange, replacement branches were sampled. Leaves were acclimated in the cuvette until a stable rate of gas exchange was recorded, typically 300+ seconds. Cuvette conditions were as follows: PAR = 1500 $\mu mol\ m^{-2}\ s^{-1}$; $C_a = 400\ \mu mol\ mol^{-1}$; leaf temperature ≈ 1^oC higher than expected mid-morning temperature. Mean vapour pressure deficit ranged from 0.5 kPa to 3.16 kPa across sites/seasons.

Leaves used for leaf gas exchange were used to determine leaf fresh mass and then oven-dried to constant mass for determination of total foliar N and P through colorimetric analyses using a flow injection system (QuikChem 8500, Lachat Instruments, Loveland, Colorado, USA).

^{13}C isotope composition of leaves

Mature, healthy, upper canopy, sunlit leaves were collected in the wet/dry or summer/winter seasons and dried in an oven at 60˚C for five days. After drying, each leaf sample was ground with a Retsch MM300 bead grinding mill (Verder Group, Netherlands) until finely and homogeneously ground. Between one and two milligrams of ground material was sub-sampled in 3.5 mm X 5 mm tin capsules for analysis of δ^{13}C giving three representative independent values per tree.

All δ^{13}C analyses were performed using a Picarro G2121-i Analyser (Picarro, Santa Clara, CA, USA) for isotopic CO_2 in the UTS TERG research laboratory. Atropine and Acetanilide were used as laboratory standard references and results were normalised with the international standards Sucrose (IAEA-CH-6, $\delta^{13}C_{VPDB}$ = -10.45 ‰), Cellulose (IAEA-CH-3, $\delta^{13}C_{VPDB}$ = -24.72 ‰) and Graphite (USGS24, $\delta^{13}C_{VPDB}$ = -16.05 ‰). δ^{13}C across all samples ranged from *ca* -25‰ to *ca* -37‰ with a measurement error (standard deviation) of 0.5 ‰.

Methodology and statistical analyses

Species-mean values (obtained from leaves sampled from four to six individuals) for the dominant overstorey species for each SuperSite were calculated for each trait to account for inter-species variability. The distribution of species means for each season was tested for non-normality (Shapiro-Wilk test, α= 0·05) and homogeneity of variances (Bartlett test). All climate variables related to temperature were approximately normally distributed and most of the precipitation related variables were log-normally distributed. Bulk-leaf Δ^{13}C values were also normally distributed. The distributions of five out of 16 leaf-traits were deemed normal and left untransformed in all subsequent analyses. Other traits showed approximately normal distribution after natural log/square-root distribution and therefore transformed appropriately. Regression analysis was performed to investigate relationships among bulk-leaf Δ^{13}C, leaf traits and MAP at the site level, where MAP was treated as an independent variable and species mean values were treated as a continuous response variable. Assumptions of the models were checked for normality and homoscedasticity of the residuals. Relationships between traits were explored by fitting standardized major axis (SMA) (Legendre & Legendre, 1998, Warton *et al.*, 2006) and slopes were fitted individually for both dry- and wet-season using the *smatr* library in R (Warton *et al.*, 2012). SMA slope-fitting techniques are appropriate for describing bivariate relationships where X as well as Y variables have variation associated with them due to measurement error and species sampling (Sokal & Rohlf, 1995). First, robust SMA regression slopes were fitted separately for dry-season and wet-season for each bivariate relationship between bulk-leaf Δ^{13}C and a leaf-trait. For a given bivariate relationship, if SMA regressions were significant for both seasons, the existence of a common slope of the relationships was tested for using a Bartlett-corrected likelihood ratio test. If the assumption of a common slope was justified, Wald tests were performed to identify significant differences in elevation between the two seasons and for significant shifts along the common fitted axis. Means of the $\Delta^{13}C$ were compared one-way ANOVA and significant differences between sites were determined by Tukey HSD tests (confidence level of 0.05). Assumptions of ANOVA were tested for normality and homoscedasticity of the residuals. All analyses were performed using R software package (R Development CORE Team, 2009).

Discrimination was calculated from the isotopic ratio of ^{13}C to ^{12}C in leaves as per Farquhar and Richards (1984):

$$\Delta^{13}\mathrm{C}\ (‰) = \frac{R_a - R_p}{R_p} = \frac{\partial^{13}C_a - \partial^{13}C_p}{1+\frac{\partial^{13}C_p}{1000}} \qquad (1)$$

Where, R_a is the $^{13}C/^{12}C$ ratio of CO_2 in air, and R_p is that of plant carbon; $\delta^{13}C_a$ is the $\delta^{13}C$ value of CO_2 in air (assumed to be -8‰) and $\delta^{13}C_p$ is that of the plant.

Leaf intrinsic water-use-efficiency (WUE_i) was calculated using the species mean $\Delta^{13}C$ based on a leaf-scale model of C3 photosynthetic isotope discrimination (Farquhar *et al.,* 1989):

$$WUE_i = \frac{C_a(b-\Delta^{13}\mathrm{C})}{1.6(b-a)} \qquad (2)$$

Here, *a*, *b* are fractionation factors (the change of ratio in molar concentrations) occurring during diffusion of CO_2 through stomata pores (4.4‰) and enzymatic carbon fixation by Rubisco plus a small component accounting for mesophyll conductance (27‰), respectively.

Results

Variation in $\Delta^{13}C$ with climatic parameters

Simple linear/logarithmic regression models were constructed (Table 3) to examine relationships of each temperature and precipitation-related variable with $\Delta^{13}C$ of corresponding season (for example, mean T of wettest quarter was positively correlated only with $\Delta^{13}C$ of the wet-season, not the dry-season). $\Delta^{13}C$ was strongly correlated with most of the precipitation-related parameters especially during the wet-season. The regression with mean annual temperature (MAT) did not adequately capture variability of $\Delta^{13}C$ across sites (dry-season: Adj r^2=0.058, $p<0.05$; wet-season, non-significant), although both dry and wet-season $\Delta^{13}C$ were significantly correlated with three other temperature related parameters; i.e. isothermality, temperature seasonality and temperature annual range (Table 3).

Variation of $\Delta^{13}C$ and WUE_i with MAP

$\Delta^{13}C$ increased with increasing MAP along the rainfall gradient for both seasons (Fig. 1, Table 3) and MAP explained 35% of variation in $\Delta^{13}C$ during both dry- and wet-season (dry-season: Adj r^2 = 0.357, $p < 0.0001$ and wet-season Adj r^2 = 0.351, $p < 0.0001$). However, the strongest relationships were observed between $\Delta^{13}C$ and precipitation of the warmest quarter during the dry-season (Adj r^2 = 0.369, $p < 0.0001$) and between $\Delta^{13}C$ and precipitation of the wettest quarter during the wet-season (Adj r^2 = 0.404, $p < 0.0001$). Relationships of leaf intrinsic water-use-efficiency (WUE_i) with MAP were similar in magnitude to that of $\Delta^{13}C$ but with a negative slope, i.e. WUE_i was significantly larger in the drier sites and smaller in the wetter sites. There was no difference in slope of the regression of $\Delta^{13}C$ nor WUE_i with MAP between seasons.

Variation in $\Delta^{13}C$ with temperature related parameters

Temperature seasonality (i.e., the difference between the annual maximum and minimum temperatures) was the strongest predictor of $\Delta^{13}C$ among the temperature related variables (dry-season: Adj r^2 = 0.400, $p < 0.0001$ and wet-season Adj r^2 = 0.487, $p < 0.0001$). After temperature seasonality, isothermality (i.e., mean day-to-night temperature oscillation relative to the mean summer-to-winter oscillation) and temperature annual range were the two strongest predictors of $\Delta^{13}C$ in the single factor linear regression models (Table 3). Temperature seasonality was a stronger predictor of variation in $\Delta^{13}C$ than MAP.

Variation of $\Delta^{13}C$ and WUE_i with annual moisture index

Although sites were sampled in dry- and wet-seasons, from a climatic point of view, wet-season at the wetter sites (e.g. in FNQ) represents very different conditions from wet-seasons at much drier sites (e.g. AMU). Site average Moisture indices (MI) from the Ozflux sites were therefore used in the analysis as an additional measure of moisture availability. Regression analysis showed significant increase in $\Delta^{13}C$ with increase in MI with larger Adj r^2 values than MAP during the wet-season (Adj r^2

= 0.375, $p<0.0001$). This relationship of MI with $\Delta^{13}C$ during the dry-season sampling, however, showed much smaller Adj r^2 values compared to MAP (Adj r^2 = 0.171, $p<0.0001$) – highlighting the seasonal differences of the relationships of $\Delta^{13}C$ with climate variables (Table 3). Similar relationships of MI and WUE_i with opposite (negative) slopes were obtained from regression analysis: significantly larger WUE_i was evident at sites with smaller MI.

Effect of seasonality of precipitation on $\Delta^{13}C$ and WUE_i

Although MAP captured a significant variation of $\Delta^{13}C$ during both seasons, the most significant positive relationship of dry-season $\Delta^{13}C$ was observed with precipitation of the warmest quarter and of wet-season $\Delta^{13}C$ was observed with precipitation of the wettest quarter (as previously described, Table 3). Furthermore, the relationships of most of the climate variables showed larger Adj r^2 values during the wet-season sampling than the dry-season sampling. These results suggest that, although MAP captures the variation of $\Delta^{13}C$ across the continent both for dry- and wet-season, $\Delta^{13}C$ is to some extent modulated by precipitation seasonality. There were no significant differences between dry- and wet-season mean $\Delta^{13}C$ and WUE_i across sites (One-way ANOVA, $p>0.05$, supplementary Fig. S3).

Variation in $\Delta^{13}C$ and WUE_i across biomes

Mean $\Delta^{13}C$ and WUE_i values grouped by biome varied significantly across both seasons (supplementary Table S4). The smallest $\Delta^{13}C$ (and largest WUE_i) occurred in semi-arid woodlands (SW; mean $\Delta^{13}C_{dry\text{-}season}$ = 19.75‰, mean $WUE_{i\ dry\text{-}season}$ = 78.14 µmol mol^{-1}; mean $\Delta^{13}C_{wet\text{-}season}$ = 19.15‰, mean $WUE_{i\ wet\text{-}season}$ = 84.6 µmol mol^{-1}) and the largest discrimination and the smallest WUE_i occurred in tropical rainforests (LTR, UTR; mean $\Delta^{13}C_{dry\text{-}season}$ = 23.42‰, mean $WUE_{i\ dry\text{-}season}$ = 31.74 µmol mol^{-1}, mean $\Delta^{13}C_{wet\text{-}season}$ = 23.64 ‰ and mean $WUE_{i\ wet\text{-}season}$ = 29.04 µmol mol^{-1}), p values <0.0001 for both seasons. Data were available only for the dry-season for the HTS biome. Variation in $\Delta^{13}C$ and WUE_i was larger across biomes during the wet-season than the dry-season (F values for wet-season=12.12 and for dry-season =7.36 from one-way ANOVA). Mean $\Delta^{13}C$ calculated for each biome were larger during the wet-season (and hence WUE_i was smaller) than the dry-season in all biomes, with the exception of semi-arid woodlands. Overall, biome type explained larger variation in $\Delta^{13}C$ (and also WUE_i) when compared to MAP (and MI) for both seasons from the ANOVA model ($\Delta^{13}C$ for MAP: Adj r^2_{MAP} = *ca*. 35%, r^2_{MI} = 40% and Adj $r^2_{biome:}$ 45% for the dry-season and 55.8% for the wet-season).

Variation in gas exchange parameters across the precipitation gradient

Species mean values of dry-season net photosynthetic assimilation (A_{400}) and stomatal conductance (g_{s400}) increased with increasing MAP (A_{400}: Adj r^2=0.224, $p<0.0001$, g_{s400}: Adj r^2= 0.414, $p<0.0001$, Fig. 2a, b). Neither of these traits was significantly correlated with MAP during the wet-season (data not shown). The ratio of A_{400} to g_{s400} (leaf intrinsic-water-use efficiency) was significantly and negatively correlated with MAP across sites during both seasons (dry-season: Adj r^2=0.458, $p<0.0001$, wet-season: Adj r^2=0.30, $p<0.0001$; Fig. 2c, d). Thus, species growing at drier sites were inherently more efficient in using water than species at wetter sites and this efficiency was larger during the dry-season than the wet-season.

Scaling relationships between $\Delta^{13}C$ and gas-exchange traits

$\Delta^{13}C$ was significantly and negatively correlated with net assimilation during the wet-season (r^2 = 0.14, $p<0.01$, slope =1.85, Fig. 3a) but not during the dry-season (r^2 = 0.03, $p> 0.05$). In contrast, $\Delta^{13}C$ correlated significantly with g_{s400} during the dry-season (r^2 = 0.07, $p<0.05$, slope =0.06, Fig. 3b) but not during the wet-season (r^2 = 0.003, $p>0.05$) and correlated negatively with vapour pressure deficit during the dry-season (r^2 = 0.23, $p<0.01$, slope =-0.19, Fig. 3c) but not during the wet-season (r^2 = 0.027, $p>0.05$). During the dry-season, significantly larger discrimination was found in species that had larger stomatal conductance and experienced smaller vapour pressure deficits. Transpiration was not significantly correlated with $\Delta^{13}C$ (data not shown).

Leaf intrinsic water-use-efficiency from gas-exchange measurements (i.e., the ratio of A_{400} to g_{s400}) was significantly correlated with $\Delta^{13}C$ during both seasons (dry-season: r^2 = 0.26, $p<0.0001$, slope=-0.17, wet-season: r^2 = 0.17, $p<0.05$, slope=-0.14, Fig. 3d) such that, species with smaller $\Delta^{13}C$ also showed significantly larger instantaneous leaf-scale measurements of WUE_i; this relationship was stronger during the dry-season than the wet-season. Standardised major axis (SMA) slopes were homogeneous between dry- and wet-seasons ($p>0.05$) with a significant shift along the axis ($p<0.05$, Table 4). Thus, the wet-season $\Delta^{13}C$ shifted towards larger values compared to the dry-season.

Scaling relationships between $\Delta^{13}C$ and leaf structural parameters

Δ^{13}C was significantly and negatively correlated with leaf mass per unit area, LMA (dry-season: r^2 = 0.31, $p<0.0001$, slope=-0.15, wet-season: r^2 = 0.43, $p<0.0001$, slope=-0.21), leaf fresh mass per unit area, FMA (dry-season: r^2 = 0.31, $p<0.0001$, slope=-0.15, wet-season: r^2 = 0.45, $p<0.0001$, slope=-0.14) and the ratio leaf dry to fresh mass, LDMC (dry-season: r^2 = 0.18, $p<0.001$, slope=-0.04, wet-season: r^2 = 0.11, $p<0.05$, slope=-0.04). Slopes did not differ between dry- and wet-season for any of these traits, i.e., LMA, FMA and LDMC ($p > 0.05$) and no significant shifts in elevation or slope were identified (Table 5). Thus, SMA was performed on the entire dataset including samples from both dry- and wet-seasons and results are presented in Fig. 4, which shows that significantly larger discrimination against ^{13}C was found in leaves with smaller LMA (Fig. 4a), smaller FMA (Fig. 4b) and smaller LDMC (Fig. 4c).

Scaling relationships between $\Delta^{13}C$ and leaf-nutrients

Of all the nutrient related parameters, Δ^{13}C significantly and negatively correlated with total leaf N expressed on an area basis during both seasons (dry-season: r^2 = 0.19, $p<0.001$, slope=-0.18, wet-season: r^2 = 0.49, $p<0.0001$, slope=-0.16). Slopes and elevation did not differ between seasons (Table 4) and thus SMA was performed on the entire dataset (Fig. 5a). Δ^{13}C was significantly and positively correlated with total leaf P expressed in mass basis only during the dry-season (Fig. 5b**,** r^2 = 0.14, $p<0.01$, slope =0.28). In contrast, total leaf P expressed in area basis was significantly correlated with Δ^{13}C only during the wet-season (Fig. 5c, r^2 = 0.38, $p<0.0001$, slope = 0.18) and larger discrimination was associated with smaller phosphorus content per unit area of leaves. No other nutrient related leaf-traits showed any significant relationship with Δ^{13}C (Table 4).

Variation of leaf traits with moisture index

In addition to MAP, bivariate linear regression was performed with moisture index (MI) treated as an independent predictor variable and all other leaf traits treated as continuous response variables. The results of these regressions are compiled in Table S3. MI was considered as another measure of water availability that also takes into account the very different *wet* conditions and temperatures experienced across different sites. The relationships of leaf-traits with MI were not different in nature than those with leaf-traits and MAP with generally slightly smaller Adj r^2 values (Table S3).

Discussion

The latest projections for Australia's near-future climate can be summarised as a continental average increase of 1 °C by 2030 (relative to 1990) and 2.2 – 5 °C increase by 2070, with reduced winter and spring rainfall across southern mainland Australia and with longer periods of drought conditions experienced (CSIRO and Bureau of Meteorology 2016). Future projections for northern monsoonal Australia remain highly uncertain. In the following discussion, we show how declines in foliar isotope discrimination and increased WUE_i with declining rainfall are larger at low rainfall sites than high rainfall sites. Furthermore, mean annual temperature was less able to predict isotope discrimination and WUE_i than temperature seasonality, isothermality and temperature annual range. Consequently, understanding these later characteristics of temperature are more important than projections of changes in annual mean temperature for improving our understanding of possible vegetation responses to such climate change. Our analyses of seasonal differences in WUE_i suggest that declines in winter and spring rainfall, where annual rainfall declines to approximately <500 mm will result in significant increases in WUE_i. We now discuss our results in detail.

Characterising climate variability with $\Delta^{13}C$

This study addresses a significant data gap of carbon isotope ratio measurements in Australian ecosystems within global compilations - providing $\Delta^{13}C$ measurements at eight sites in Australia and across a large number of families and genera sampled both during the wet- and the dry-season. Notwithstanding the potential for additional factors, including changes in mesophyll conductance, post photosynthetic discrimination and leaf life-span, to influence $\delta^{13}C$ (and therefore $\Delta^{13}C$; Farquhar *et al.,* 1982; Evans and Caemmerer 1996; Seibt *et al.,* 2008) we never-the-less conclude that $\Delta^{13}C$ is a powerful tool for characterising variability in climate and the response of WUE_i across continental Australia.

Significant positive relationships were observed between bulk-leaf $\Delta^{13}C$ (and hence a strong negative relationship of WUE_i), and MAP during both seasons and between $\Delta^{13}C$ and a moisture index especially during the wet-season. Smaller discrimination (18-20 ‰) and larger WUE_i (80-100 µmol/mol) values were essentially restricted to sites with MAP <350 mm yr^{-1}. This trend noticeably "flattens" as MAP increases from 900 mm yr^{-1} to 5,700 mm yr^{-1}, indicating that isotopic discrimination in wet environments remained nearly constant. Australian rainforests support 10% of Australian flora despite of occurring in only 0.2% its landmass - consequently, larger number of data points came from the wetter end of the MAP spectrum despite sampling all the dominant species at each site. Although there were fewer dominant overstorey species in the drier sites, up to 3.7‰

differences in $\Delta^{13}C$ (during dry-season sampling) and 4.5‰ differences (during wet-season sampling) among different climate biomes were apparent (Table S4). Previous smaller regional studies in southern Queensland (Stewart *et al.*, 1995), in South Africa (Midgley *et al.,* 2004) and globally (Diefendorf *et al.*, (2010) recorded similar relationships between $\Delta^{13}C$ and MAP as observed in the present study. By contrast, Cernusak *et al.*, (2011), Miller *et al.*, (2001), Schulze *et al.*, (1998) observed flat community-level responses of $\Delta^{13}C$ to MAP gradients in northern Australia. Cernusak *et al.*, (2011) concluded that non-significant relationships of $\Delta^{13}C$ with MAP resulted from a nearly constant C_i/C_a ratio observed in the closely related genera of *Eucalyptus* and *Corymbia*, the focus of most Australian studies. An increase in C_i/C_a with increasing MAP (Wright *et al.*, 2001) can therefore explain a strong response of $\Delta^{13}C$ with MAP (Stewart *et al.*, 1995). In the present study a significant relationship of C_i/C_a was identified during dry- and wet-seasons (Fig. S4) across a 22-fold increase in MAP, resulting in a strong response of $\Delta^{13}C$ to MAP.

Diefendorf *et al.*, (2010) and Kohn (2010) demonstrate in their meta-analyses the importance of variation in MAP across sites in explaining variation in foliar $\Delta^{13}C$, with only a minor role for temperature apparent in Diefendorf *et al.,* (2010). Similarly, Grossiord *et al.,* (2017) experimentally demonstrated that for *Pinus edulis*, changes in water availability have much larger impacts on growth and physiology than changes in temperature. In contrast, Moles et al., (2014) demonstrated that mean annual temperature (MAT) was significantly more strongly correlated with plant traits than MAP. In our analyses, temperature-related climate variables were more strongly correlated with variation in foliar $\Delta^{13}C$ than MAP or MI (Table 3), reflecting the possibility that temperature related variables may be capturing effects of temperature-associated changes in vapour pressure on $\Delta^{13}C$. We conclude that future changes in temperature-related variables (e.g. seasonality and annual range) may result in larger changes in $\Delta^{13}C$ than changes in MAP, especially where MAP remains moderate-to-high.

Seasonal differences in $\Delta^{13}C$

An additional explanation for presence/absence of a strong response of $\Delta^{13}C$ with MAP relies on differences in seasonality of rainfall for north *versus* east Australian rainfall gradients (Cernusak *et al.*, 2011, Miller *et al.*, 2001). Rainfall in monsoonal northern Australia shows a strong regular seasonal distribution every year. In contrast, rainfall in eastern Australia is more evenly distributed throughout the year. In the present study, measurements of $\Delta^{13}C$ and other leaf-traits were made separately during dry- and wet-seasons and regression analyses were performed separately for each season. Although mean annual precipitation (and moisture index) adequately captured variation of

$\Delta^{13}C$ across the continent, the response of $\Delta^{13}C$ was modulated by precipitation seasonality. A stronger relationship of dry-season $\Delta^{13}C$ with precipitation of the warmest quarter and of wet-season $\Delta^{13}C$ with precipitation of the wettest quarter than their individual relationship with MAP suggest that seasonality influenced these relationships at least to the extent of species examined in this study. Furthermore, temperature seasonality, isothermality and temperature annual range among the temperature related variables were stronger predictors of $\Delta^{13}C$ compared to mean annual temperature. For the same species sampled during both seasons, stronger relationships of $\Delta^{13}C$ was consistently observed during the wet-season compared to the dry-season with most of the climate variables and MI (Table 3). Larger $\Delta^{13}C$ (and hence smaller WUE_i) during the wetter periods reflect the impact of enhanced stomatal opening during the wet-season. The smallest increase in community-averaged $\Delta^{13}C$ of the wet- from the dry-season occurred at the central Australian arid site (AMU) as was expected from the flat responses of $\Delta^{13}C$ to increasing water availability in northern Australia (Cernusak *et al.*, 2011, Miller *et al.*, 2001, Schulze *et al.*, 1998), although Schulze *et al.*, (1998) did record a response of $\Delta^{13}C$ to MAP in northern Australia for sites that were outside of the zone of influence of the monsoonal rains and where conditions were inherently drier. In contrast with AMU, the largest increase in community-averaged $\Delta^{13}C$ of the wet- compared to the dry-season occurred at the WR (Warra Tall Eucalypt) site which experiences smaller seasonality of precipitation (Table S4).

Bulk-leaf $\Delta^{13}C$ is modulated by C_i/C_a at the time when leaf dry-matter was synthesized. This raises the question: do patterns in $\Delta^{13}C$ provide information about C_i/C_a only during favourable conditions in the wet-season when canopy photosynthesis is the most active, or does it provide information about year-round variation in C_i/C_a along the precipitation gradient? This question can be addressed if $\Delta^{13}C$ values from both dry- and wet-season can be compared in addition to complementary information provided by instantaneous gas-exchange measurements. $\Delta^{13}C$ showed stronger and significant relationships with all eight precipitation variables and moisture index during the wet-season compared to the dry-season. Therefore, growing-season $\Delta^{13}C$ more reliably predicts the influence of water availability. Similar results were observed by Schulze *et al.*, (1998), who demonstrated that $\Delta^{13}C$ was about 2‰ lower in young leaves than in expanded leaves, but this value did not change any further between fully expanded fresh leaves and old leaves that had experienced a full dry-season. They concluded that, $\Delta^{13}C$ represented the conditions during the growing season rather than the conditions over the whole year, even though leaves start sprouting at the end of the dry-season, with deciduous species being earlier than evergreens.

Relative contribution of assimilation and stomatal conductance to $\Delta^{13}C$

For C_3 plants, where $\Delta^{13}C$ is primarily controlled by C_i/C_a , coordination between stomatal conductance, photosynthesis and leaf area adjustments tends to constrain the potential environmentally-driven range of $\Delta^{13}C$ (Cernusak *et al.*, 2013). Can we quantify the relative contribution of changes in photosynthesis and stomatal conductance to variation in C_i/C_a ratio? During the dry-season, $\Delta^{13}C$ correlated significantly with g_{s400} but not with A_{400}. However, during the wet-season, $\Delta^{13}C$ correlated significantly with A_{400} but not with g_{s400}. The C_i/C_a ratio was significantly correlated with g_{s400} during both seasons. Strong positive relationships of g_{s400} and C_i/C_a with MAP (data not shown; $p<.0001$ in both cases) and a weak but significant relationship of g_{s400} with $\Delta^{13}C$ ($p < 0.05$) *only* during the dry-season suggests that during the dry-season, C_i/C_a (and therefore, $\Delta^{13}C$ and WUE_i) were more strongly regulated by stomatal conductance than photosynthetic capacity. Similarly, Cernusak *et al.*, (2011) concluded that changes in photosynthetic capacity per unit leaf area between the wet- and dry-season were unlikely to account for seasonal changes in rates of photosynthesis. However, during the wet-season, a significant relationship between A_{400} and $\Delta^{13}C$ (Fig. 3a) and an apparent lack of relationship between $\Delta^{13}C$ and g_{s400} during wet-season in spite of a highly significant relationship between C_i/C_a and g_{s400} (data now shown) suggest that photosynthetic capacity more strongly regulates the $\Delta^{13}C$ signal than stomatal conductance when canopy photosynthesis is most active under favourable condition of water availability.

$\Delta^{13}C$, leaf morphology and other leaf traits

We found that leaf morphology at site/species level reflects environmental constraints on plant growth. Reduced water availability results in thicker and/or denser leaf tissues (Abrams *et al.*, 1994, Groom & Lamont, 1997, Lamont *et al.*, 2002, Witkowski *et al.*, 1992). Species with thicker and denser leaves occur where less water is available (Abrams *et al.*, 1994, Reich *et al.*, 1999). Similarly, less discrimination against ^{13}C occurs in response to reduced water availability due to increased stomatal regulation. Here we showed that $\Delta^{13}C$ was most strongly and inversely correlated with LMA among all leaf attributes considered, across both seasons, reflecting either decreased stomatal conductance or a lower C_i/C_a arising from the larger demand for CO_2 per unit leaf area arising from thicker leaves, or a reduced mesophyll conductance associated with thicker leaves (Lamont *et al.*, 2002).

Among the leaf nutrient traits, leaf N_{mass} showed significant positive relationships with MAP during both seasons and MI only during the wet-season (Table S3). However, this was not correlated with $\Delta^{13}C$. Leaf P_{mass} showed significant positive relationship with MAP and $\Delta^{13}C$ only during dry-season and no relationship with MI was identified (Table S3). In contrast, Leaf N_{area} showed significant negative relationships with both MAP and MI (Table S3) and was also correlated with $\Delta^{13}C$ during both seasons. Leaf P_{area} showed significant negative relationships with MAP during the wet-season and MI during both seasons (Table S3) and was correlated negatively with $\Delta^{13}C$ only during the wet-season. For all these traits, the nature of significant positive or negative relationships obtained from bivariate linear regression of $\Delta^{13}C$ with MAP and MI indicated that $\Delta^{13}C$ at the species level reliably reflects the water status of the site. The lack of relationship between mass based foliar nitrogen concentration and $\Delta^{13}C$ was consistent with results of Schulze *et al.*, (1998). Thus we conclude that water availability and temperature (and not foliar nutrient content) are the principal factors directly influencing $\Delta^{13}C$ across the Australian continent, in agreement with smaller-scale regional studies (Lamont *et al.*, 2002, Schulze *et al.*, 1998). The significant relationships with $\Delta^{13}C$ obtained from nutrients expressed as area basis agree with previous observations of relationships of $\Delta^{13}C$ with C_i/C_a (Cernusak *et al.*, 2013) and N_{area}; a lack of relationship on a mass basis may result from strong association between $\Delta^{13}C$ and LMA (Lamont *et al.*, 2002).

Acknowledgements

We gratefully acknowledge the financial support of the Australian Research Council through a Discovery grant awarded to DE and OKA. The project was made possible, in part, by a TERN Supplemental grant to OKA. We also are indebted to the provision of leaf samples for foliar ^{13}C analyses provided by the CIs of all the sites used in this study, including those from the Australian Terrestrial Ecosystem Research Network (TERN).

References

Abrams MD, Kubiske ME, Mostoller SA (1994) Relating wet and dry year ecophysiology to leaf structure in contrasting temperate tree species. *Ecology,* **75**, 123-133.

Ainsworth EA, Rogers A (2007) The response of photosynthesis and stomatal conductance to rising [CO_2]: mechanisms and environmental interactions. *Plant, Cell & Environment,* **30**, 258-270.

Bowman DM, Walsh A, Milne DJ (2001) Forest expansion and grassland contraction within a *Eucalyptus* savanna matrix between 1941 and 1994 at Litchfield National Park in the Australian monsoon tropics. *Global Ecology and Biogeography,* **10**, 535-548.

Brugnoli E, Farquhar GD (2000) Photosynthetic fractionation of carbon isotopes. In: *Advances in Photosynthesis and Respiration*, Springer, Neherlands, 399-434.

Cernusak LA, Hutley LB, Beringer J, Holtum JA, Turner BL (2011) Photosynthetic physiology of eucalypts along a sub-continental rainfall gradient in northern Australia. *Agricultural and Forest Meteorology,* **151**, 1462-1470.

Cernusak LA, Ubierna N, Winter K, Holtum JaM, Marshall JD, Farquhar GD (2013) Environmental and physiological determinants of carbon isotope discrimination in terrestrial plants. *New Phytologist,* **200**, 950-965.

Cleverly J, Eamus D, Van Gorsel E *et al.* (2016) Productivity and evapotranspiration of two contrasting semiarid ecosystems following the 2011 global carbon land sink anomaly. *Agricultural and Forest Meteorology*, 220: 151-159.

CSIRO and Bureau of Meteorology (2016) State of the Climate 2016. Technical Report, CSIRO and Bureau of Meteorology, Australia. 220 pp.

Cunningham SA, Summerhayes B, Westoby M (1999) Evolutionary divergences in leaf structure and chemistry, comparing rainfall and soil nutrient gradients. *Ecological Monographs,* **69**, 569-588.

Dawson TE, Mambelli S, Plamboeck AH, Templer PH, Tu KP (2002) Stable isotopes in plant ecology. *Annual Review of Ecology and Systematics,* **23**, 507-559.

Diefendorf AF, Mueller KE, Wing SL, Koch PL, Freeman KH (2010) Global patterns in leaf C discrimination and implications for studies of past and future climate. *Proceedings of the National Academy of Sciences,* **107**, 5738-5743.

Dragoni D, Caylor K, Schmid H (2009) Decoupling structural and environmental determinants of sap velocity: Part II. Observational application. *Agricultural and Forest Meteorology,* **149**, 570-581.

Eamus D, Hatton T, Cook P, Colvin C (2006) *Ecohydrology: vegetation function, water and resource management*, CSIRO Publishing: Melbourne.

Eamus D, Huete A, Yu Q (2016) Vegetation Dynamics: A synthesis of plant ecophysiology, remote sensing and modelling. Cambridge University Press, Cambrdige UK, pp517.

Evans JR, von Caemmerer S (1996). CO_2 diffusion inside leaves. *Plant Physiology* **110**, 339-346.

Farquhar GD (1991) Use of stable isotopes in evaluating plant water use efficiency. In: *Stable isotopes in plant nutrition, soil fertility and environmental studies.* Proceedings of a symposium, Vienna, 475-488.

Farquhar GD, Ehleringer JR, Hubick KT (1989) Carbon isotope discrimination and photosynthesis. *Annual Review of Plant Physiology and Plant Molecular Biology,* **40**, 503-537.

Farquhar GD, O'Leary MH, Berry JA (1982) On the relationship between carbon isotope discrimination and the intercellular carbon dioxide concentration in leaves. *Functional Plant Biology,* **9**, 121-137.

Farquhar GD, Richards RA (1984) Isotopic composition of plant carbon correlates with water-use efficiency of wheat genotypes. *Australian Journal of Plant Physiology,* **11**, 539-552.

Fonseca CR, Overton JM, Collins B, Westoby M (2000) Shifts in trait-combinations along rainfall and phosphorus gradients. *Journal of Ecology,* **88**, 964-977.

Gosper CR, Prober SM, Yates CJ, Wiehl G (2013) Estimating the time since fire of long-unburnt *Eucalyptus salubris* (Myrtaceae) stands in the Great Western Woodlands. *Australian Journal of Botany,* **61**, 11-21.

Groom P, Lamont BB (1997) Xerophytic implications of increased sclerophylly: interactions with water and light in *Hakea psilorrhyncha* seedlings. *New Phytologist,* **136**, 231-237.

Grossiord C, Sevanto S, Adams HD, Collins AD, Dickman LT, McBranch N, Michaletz ST, Stockton EA, Vigil M, McDowell NG (2017). Precipitation, not air temperature, drives functional responses of trees in semi-arid ecosystems. *Journal of Ecology* **105**, 163-175.

Hickey JE, Su W, Rowe P, Brown MJ, Edwards L (1999) Fire history of the tall wet eucalypt forests of the Warra ecological research site, Tamania. *Australian Forestry,* **62**, 66-71.

Hijmans RJ, Cameron SE, Parra JL, Jones PG, Jarvis A (2005) Very high resolution interpolated climate surfaces for global land areas. *International Journal of Climatology,* **25**, 1965-1978.

Hutley LB, Beringer J (2010) Disturbance and climatic drivers of carbon dynamics of a north Australian tropical savanna. In: *Ecosystem function in savannas: measurement and modeling at landscape to global scales.* CRC Press, Boca Raton, 57-75.

Koch GW, Vitousek PM, Steffen WL, Walker BH (1995) Terrestrial transects for global change research. *Vegetatio,* **121**, 53-65.

Kohn MJ (2010) Carbon isotope compositions of terrestrial C3 plants as indicators of (paleo) ecology and (paleo) climate. *Proceedings of the National Academy of Sciences,* **107**, 19691-19695.

Lambers H, Poorter H (1992) Inherent variation in growth rate between higher plants: a search for physiological causes and ecological consequences. In: *Advances in Ecological Research,* **23**, 187-261.

Lamont BB, Groom PK, Cowling R (2002) High leaf mass per area of related species assemblages may reflect low rainfall and carbon isotope discrimination rather than low phosphorus and nitrogen concentrations. *Functional Ecology,* **16**, 403-412.

Legendre P, Legendre L (1998) *Numerical Ecology,* Elsevier: Amsterdam, The Netherlands.

Livingston NJ, Spittlehouse DL (1996) Carbon isotope fractionation in tree ring early and late wood in relation to intra-growing season water balance. *Plant Cell and Environment,* **19**, 768-774.

Lu XJ, Wang YP, Wright IL et al., 2017 Incorporation of plant traits in a land surface model helps explain the global biogeographical distribution of major forest functional types. *Global* Ec*ology and Biogeography*, **26**, 304-317.

Medlyn BE, Duursma RA, Eamus D *et al.* (2011) Reconciling the optical and empirical approaches to modelling stomatal conductance. *Global Change Biology,* **17**, 2134-2144.

Meyer WS, Kondrlovà E, Koerber GR (2015) Evaporation of perennial semi-arid woodland in southeastern Australia is adapted for irregular but common dry periods. *Hydrological Processes,* **29**, 3714-3726.

Midgley GF, Aranibar JN, Mantlana KB, Macko S (2004) Photosynthetic and gas exchange characteristics of dominant woody plants on a moisture gradient in an African savanna. *Global Change Biology,* **10**, 309-317.

Miller JM, Williams RJ, Farquhar GD (2001) Carbon isotope discrimination by a sequence of Eucalyptus species along a subcontinental rainfall gradient in Australia. *Functional Ecology,* **15**, 222-232.

Moles AT, Perkins SE, Shawn W et al., (2014). Which is a better predictor of plant traits: temperature or precipiation? *Journal of Vegetation Science* 25, 1167-1180.

Murphy BP, Russel-Smith J, Prior LD (2010) Frequent fires reduce tree growth in northern Australian savannas: implications for tree demography and carbon sequestration. *Global Change Biology,* **16**, 331-343.

R Development Core Team (2009) R: A Language and Environment for Statistical Computing. Vienna, Austria.

Reich P, Walters M, Ellsworth D (1992) Leaf life-span in relation to leaf, plant, and stand characteristics among diverse ecosystems. *Ecological Monographs,* **62**, 365-392.

Reich PB, Ellsworth DS, Walters MB, Vose JM, Gresham C, Volin JC, Bowman WD (1999) Generality of leaf trait relationships: a test across six biomes. *Ecology,* **80**, 1955-1969.

Rossatto DR, Silva LDCR, Villalobos-Vega R, Sternberg LDSL, Franco AC (2012) Depth of water uptake in woody plants relates to groundwater level and vegetation structure along a topographic gradient in a neotropical savanna. *Environmental and Experimental Botany,* **77**, 259-266.

Schulze ED, Kelliher FM, Korner C, Lloyd J, Leuning R (1994) Relationships among maximum stomatal conductance, ecosystem surface conductance, carbon assimilation rate, and plant nitrogen nutrition: a global ecology scaling exercise. *Annual Review of Ecology and Systematics,* **25**, 629-660.

Schulze ED, Mooney HA, Sala OE *et al.* (1996) Rooting depth, water availability, and vegetation cover along an aridity gradient in Patagonia. *Oecologia,* **108**, 503-511.

Schulze ED, Turner NC, Nicolle D, Schumacher J (2006) Leaf and wood carbon isotope ratios, specific leaf areas and wood growth of *Eucalyptus* species across a rainfall gradient in Australia. *Tree Physiology,* **26**, 479-492.

Schulze ED, Williams RJ, Farquhar GD, Schulze W, Langridge J, Miller JM, Walker BH (1998) Carbon and nitrogen isotope discrimination and nitrogen nutrition of trees along a rainfall gradient in northern Australia. *Functional Plant Biology,* **25**, 413-425.

Seibt U, Rajabi A, Griffiths H, Berry J (2008) Carbon isotopes and water-use efficiency: sense and sensitivity. *Oecologia* **155**, 441-454.

Sokal RR, Rohlf FJ (1995) *Biometry: the principles and practice of statistics in biological research,* W.H. Freeman & Co., San Francisco.

Stewart GR, Turnbull M, Schmidt S, Erskine P (1995) ^{13}C natural abundance in plant communities along a rainfall gradient: a biological integrator of water availability. *Functional Plant Biology,* **22**, 51-55.

Taylor D, Eamus D (2008) Coordinating leaf functional traits with branch hydraulic conductivity: resource substitution and implications for carbon gain. *Tree Physiology,* **28**, 1169-1177.

Turner IM (1994) A quantitative analysis of leaf form in woody plants from the world's major broadleaved forest types. *Journal of Biogeography,* **21**, 413-419.

Turner NC, Schulze ED, Nicolle D, Schumacher J, Kuhlmann I (2008) Annual rainfall does not directly determine the carbon isotope ratio of leaves of *Eucalyptus* species. *Physiologia Plantarum,* **132**, 440-445.

Verheijen LM, Brovkin V, Aerts R et al., (2013) Impacts of trait variation through observed trait-climate relationships on performance of an Earth system model: a conceptual analysis. *Biogeosciences* **10**, 5497-5515.

Warton DI, Duursma RA, Falster DS, Taskinen S (2012) smatr 3–an R package for estimation and inference about allometric lines. *Methods in Ecology and Evolution,* **3**, 257-259.

Warton DI, Wright IJ, Falster DS, Westoby M (2006) Bivariate line-fitting methods for allometry. *Biological Reviews,* **81**, 259-291.

Weerasinghe LK, Creek D, Crous KY, Xiang S, Liddell MJ, Turnbull MH, Atkin OK (2014) Canopy position affects the relationships between leaf respiration and associated traits in a tropical rainforest in Far North Queensland. *Tree Physiology,* **34**, 564-584.

Werner C, Schnyder H, Cuntz M *et al.* (2012) Progress and challenges in using stable isotopes to trace plant carbon and water relations across scales. *Biogeosciences,* **9**, 3083-3111.

Whitley R, Taylor D, Macinnis-Ng C *et al.* (2013) Developing an empirical model of canopy water flux describing the common response of transpiration to solar radiation and VPD across five contrasting woodlands and forests. *Hydrological Processes,* **27**, 1133-1146.

Whittaker RH (1975) *Communities and ecosystems, 2nd edition*. Macmillan Publishing Company*,* New York.

Witkowski E, Lamont B, Walton C, Radford S (1992) Leaf demography, sclerophylly and ecophysiology of two *Banksias* with contrasting leaf life spans. *Australian Journal of Botany,* **40**, 849-862.

Wright IJ, Reich PB, Cornelissen JHC *et al*., (2005) Modulation of leaf economic traits and trait relationships by climate. *Global Ecology and Biogeography,* **14**, 411-421.

Wright IJ, Reich PB, Westoby M (2001) Strategy shifts in leaf physiology, structure and nutrient content between species of high-and low-rainfall and high-and low-nutrient habitats. *Functional Ecology,* **15**, 423-434.

Wright IJ, Reich PB, Westoby M *et al.* (2004) The worldwide leaf economics spectrum. *Nature,* **428**, 821-827.

Zeppel M, Macinnis-Ng C, Palmer A *et al.* (2008) An analysis of the sensitivity of sap flux to soil and plant variables assessed for an Australian woodland using a soil–plant–atmosphere model. *Functional Plant Biology,* **35**, 509-520.

Zolfaghar S, Villalobos-Vega R, Cleverly J, Zeppel M, Rumman R, Eamus D (2014) The influence of depth-to-groundwater on structure and productivity of *Eucalyptus* woodlands. *Australian Journal of Botany,* **62**, 428-437.

Zhuang W, Cheng L, Whitley R, et al., (2016) How energy and water availability constrain vegtetation water-use along the North Australian Tropical Transect. *International Journal of Plant Production*, **10**, 403-424.

Figure captions

Figure 1: **Carbon isotope discrimination in leaf dry-matter ($\Delta^{13}C$, panels a, b) and leaf intrinsic water-use-efficiency calculated from $\Delta^{13}C$ (WUE_i, panels c, d) plotted as a function of mean annual precipitation (MAP).**

Grey and black symbols represent sampling for dry (left panels) and wet-season (right panels) respectively- each symbol representing the species mean of four to six individuals. Error bars represent standard errors.

Figure 2: **Net assimilation, A_{400}, stomatal conductance, g_{s400} (square-root transformed) and leaf intrinsic water-use-efficiency (A_{400}/g_{s400}) plotted as functions of mean annual precipitation (MAP).**

Statistically significant relationships with MAP are plotted with red regression lines. Each symbol represents the species mean of four to six individuals. Error bars are one standard error (not shown when data were transformed due to non-normality).

Figure 3: **Scaling relationships between $\Delta^{13}C$ and (a) Net assimilation, (b) stomatal conductance, (c) vapour pressure deficit and (d) ln (A_{400}/g_{s400}).**

Data from dry- and wet-season sampling are shown in grey and black circles respectively. Only statistically significant slopes from SMA are plotted with red lines. Non-significant SMA slopes are not shown. In (a) the wet-season regression is significant; in (b) and (c) the dry-season regressions are significant; in (d) both season regressions are significant.

Figure 4: **Scaling relationships between $\Delta^{13}C$ and (a) leaf mass per unit area, (b) fresh mass per unit area (FMA) and (c) ratio leaf dry mass to fresh mass.**

Dry-season samples are represented by grey circles and the wet-season samples by black circles. Statistically significant slopes from SMA are plotted with red lines. A single regression describes both seasons in all three relationships.

Figure 5: **Scaling relationships between $\Delta^{13}C$ and (a) total leaf N expressed in area basis, Leaf N_{area}, (b) total leaf P expressed in mass basis, Leaf P_{mass} and (c) total leaf P expressed in area basis, Leaf P_{area}.**

Dry-season samples are represented by grey circles and dashed lines and wet-season samples by black circles and solid lines. Statistically significant slopes from SMA are plotted with red lines. Non-significant SMA slopes are not shown. In (a) a single regression describes both seasons. In (b) only the dry-season regression is significant. In (c) only the wet-season regression is significant.

Table 1: **Site Characteristics**

Name, latitude, longitude, mean annual precipitation, mean annual temperature and biome descriptions for SuperSites studied across the continent. Long term average climate data were obtained from the WorldClim database.

Site / Abbreviation	Lat °	Long °	MAP (mm)	MAT (°C)	Biome / Abbreviation
Calperum Mallee /CM	-34.0373	140.6738	255	17.3	Semi-arid woodland / SW
Great Western Woodlands / GWW	-30.2640	120.6917	273	18.5	Temperate woodland /TW
Alice Mulga	-22.2828	133.2493	321	22.4	Semi-arid tropical savanna / STS
Cumberland Plain	-33.6190	150.7382	900	17.7	Temperate woodland / TW
Warra Tall Eucalypt	-43.0888	146.6512	1474	10.1	Temperate wet forest / TWF
Litchfield Savanna*	-12.4853	131.1461	1714	27.8	High rainfall tropical savanna / HTS
FNQ - Robson Creek†	-17.1195	145.6323	2140	21.0	Upland wet tropical rainforest /UTR
FNQ - Cape Tribulation†	-16.1000	145.4500	5700	25.2	Lowland wet tropical rainforest / LTR

*Data from Cernusak *et al.*, (2011) for Howard Springs was used as a representative of Litchfield Savanna site.

†Data were collected from two nodes for the Far North Queensland (FNQ) rainforests SuperSites. OzFlux site average data was used for the Cape Tribulation node in all analysis.

Table 2: **List of leaf-traits examined in this study**

Abbreviation	Units	Leaf-traits
A_{400}	µmol CO_2 m^{-2} s^{-1}	Light-saturated net assimilation at an atmospheric [CO_2] of 400 ppm
E_{400}	mmol H_2O m^{-2} s^{-1}	Transpiration rate at [CO_2] 400 ppm under light saturation
$vpdL_{400}$	KPa	Vapour pressure deficit based on leaf temp
g_s400	mmol H_2O m^{-2} s^{-1}	Stomatal conductance at [CO_2] 400 ppm with light saturation
C_i/C_a	-	Intercellular [CO_2] : ambient [CO_2]
C_{i400}	µmol CO_2 mol^{-1}	Intercellular [CO_2] with CO_2 reference at 400 ppm and light saturation
LDMC	-	Ratio leaf dry to fresh mass
LMA	g m^{-2}	Leaf mass per unit area
FMA	g m^{-2}	Fresh mass per unit area
Leaf N_{mass}	mg g^{-1}	Total leaf [N]
Leaf P_{mass}	mg g^{-1}	Total leaf [P]
RatioNP	-	Ratio of total leaf [N] : [P]
Leaf N_{area}	mg m^{-2}	Total leaf [N], (area basis)
Leaf P_{area}	mg m^{-2}	Total leaf [P], (area basis)
PNUE	µmol CO_2 s^{-1} g^{-1} N	Photosynthetic nitrogen use efficiency (Net assimilation at [CO_2] 400 ppm, per unit N)
PPUE	µmol CO_2 s^{-1} g^{-1} P	Photosynthetic phosphorus use efficiency (Net assimilation at [CO_2] 400 ppm, per unit P)
$\delta^{13}C$	‰	Deviation of foliar ^{13}C from a standard
$\Delta^{13}C$	‰	Calculated foliar discrimination against ^{13}C

Table 3: **Relationships of Δ^{13}C with climate parameters**

Δ^{13}C of dry and wet-season correlated with temperature and precipitation parameters of corresponding season. MI was calculated for each site from OZFlux site average data.

Variables	Dry-season		Wet-season	
	Adj r^2	slope	Adj r^2	slope
Mean Annual Temperature	0.058$^{\bullet}$	+	0.015	NS
Mean Diurnal Range	0.201***	-	0.380***	-
Isothermality	0.394***	+	0.356***	+
Temperature Seasonality	0.400***	-	0.487***	-
Max T (Warmest Month)	0.016	NS	0.141**	-
Min T (Coldest Month)	0.198***	+	0.134**	+
T Annual Range	0.308***	-	0.434***	-
Mean T (Wettest Quarter)	N/A	N/A	0.147**	+
Mean T (Driest Quarter)	0.049$^{\bullet}$	+	N/A	N/A
Mean T (Warmest Quarter)	-0.011	NS	-0.013	NS
Mean T (Coldest Quarter)	0.153**	+	0.107*	+
ln Mean Annual Precipitation	0.357***	+	0.351***	+
ln Precip. (Wettest Month)	N/A	N/A	0.393***	+
ln Precip. (Driest Month)	0.246***	NS	N/A	N/A
Precip. (Seasonality)	0.318***	+	0.366***	+
ln Precip. (Wettest Quarter)	N/A	N/A	0.404***	+
ln Precip. (Driest Quarter)	0.228**	NS	N/A	N/A
ln Precip. (Warmest Quarter)	0.369***	+	0.389***	+
ln Precip. (Coldest Quarter)	0.114**	NS	0.393***	+
ln Moisture index (ratio of precipitation to potential evaporation)	0.171***	+	0.375***	+

***p<0.0001, **p<0.001, *p<0.01, $^{\#}$p<0.05, NS=non-significant, N/A= not analysed.

Table 4: Scaling relationships between bulk-leaf Δ^{13}C and other leaf attributes

Trait correlated with Δ^{13}C	**Season**				**Statistical tests**					
	Dry		**Wet**		**Bartlett's likelihood ratio test for a common slope**		**Wald tests**			
							Shift along common elevation		**Shift along common fitted slope**	
	r^2	**Slope**	**r^2**	**slope**	**Y/N**	**p**	**Y/N**	**p**	**Y/N**	**p**
A$_{400}$	0.006	1.852	0.135*	-1.514	-	-	-	-	-	-
Ln A$_{400}$/gs$_{400}$	0.259***	-0.169	0.172$^{\bullet}$	-0.131	Y	0.234	N	0.837	Y	0.04
C$_i$/C$_a$	0.198**	0.060	0.191**	0.036	N	0.017	-	-	-	-
C$_i$400	0.187**	22.199	0.258**	14.088	N	0.044	-	-	-	-
A$_{400}$ ~ C$_i$/C$_a$	0.025	30.419	0.008	40.750	-	-	-	-	-	-
sqrt g$_{s400}$ ~ C$_i$/C$_a$	0.216**	0.911	0.317***	1.211	Y	0.105	N	0.602	N	0.138
sqrt g$_{s400}$	0.072$^{\bullet}$	0.055	0.003	-0.045	-	-	-	-	-	-
Ln E$_{400}$	0.0005	-0.336	0.005	-0.265	-	-	-	-	-	-
Ln vpdL$_{400}$	0.229**	-0.187	0.027	-0.146	-	-	-	-	-	-
LDMC	0.177**	-0.038	0.113$^{\bullet}$	-0.038	Y	0.142	N	0.566	N	0.093
Ln LMA	0.306***	-0.189	0.433***	-0.206	Y	0.632	N	0.663	N	0.168
Ln FMA	0.307***	-0.148	0.445***	-0.144	Y	0.867	N	0.702	N	0.071
Ln Leaf N$_{mass}$	0.030	0.188	0.010	0.134	-	-	-	-	-	-
Ln Leaf P$_{mass}$	0.135*	0.280	0.003	0.171	-	-	-	-	-	-
Ln Ratio NP	0.105	-0.212	0.004	0.091	-	-	-	-	-	-
Ln Leaf N$_{area}$	0.191***	-0.176	0.493**	-0.161	Y	0.616	N	0.109	N	0.423
Ln Leaf P$_{area}$	0.002	-0.181	0.379***	0.184	-	-	-	-	-	-
PNUE	0.037	0.838	0.025	0.703	-	-	-	-	-	-
Ln PPUE	0.0002	-0.301	0.016	0.229	-	-	-	-	-	-

***p<0.0001, **p<0.001, *p<0.01, $^{\bullet}$p<0.05, Y indicates existence if a common slope in which case Wald tests were performed.

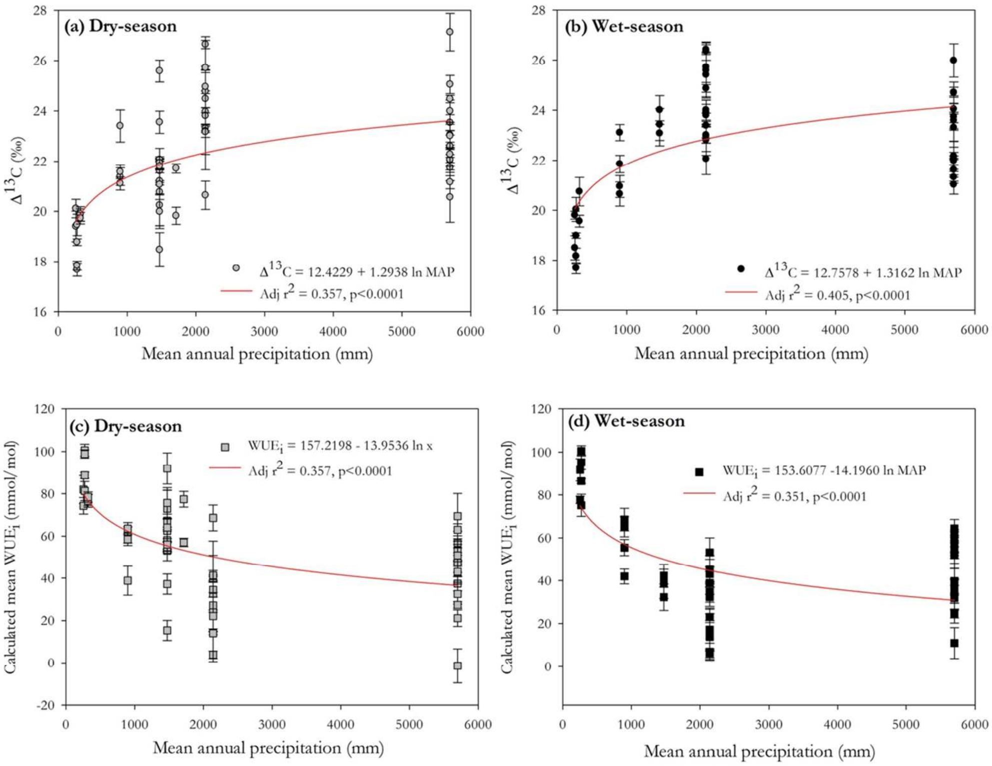

135x108mm (300 x 300 DPI)

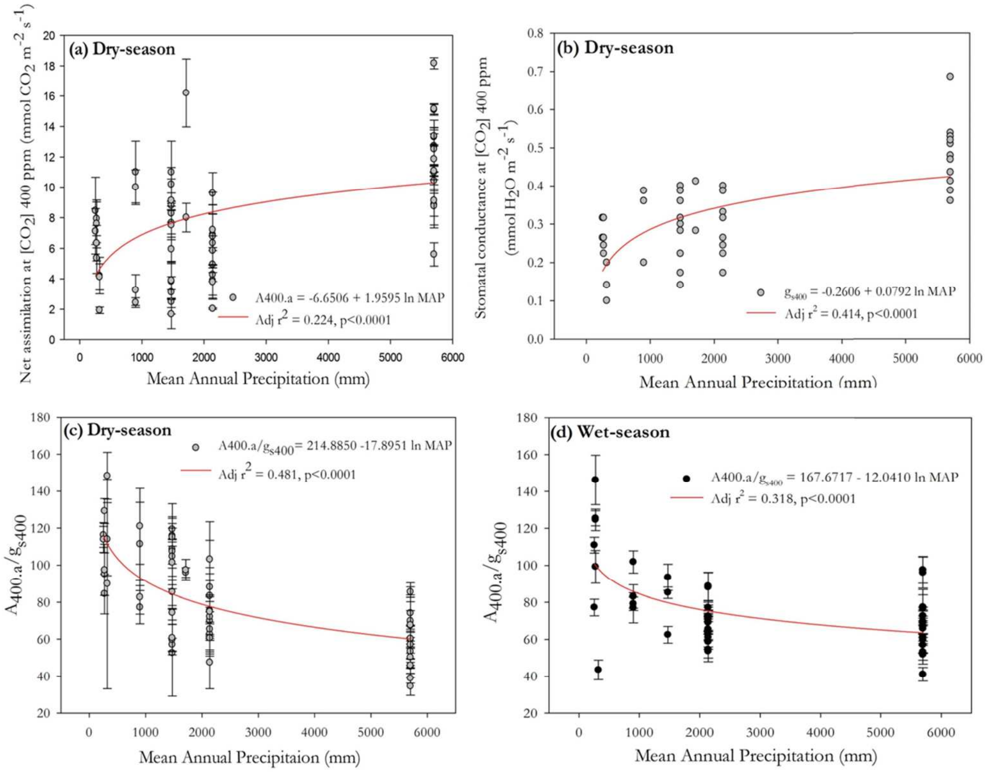

131x102mm (300 x 300 DPI)

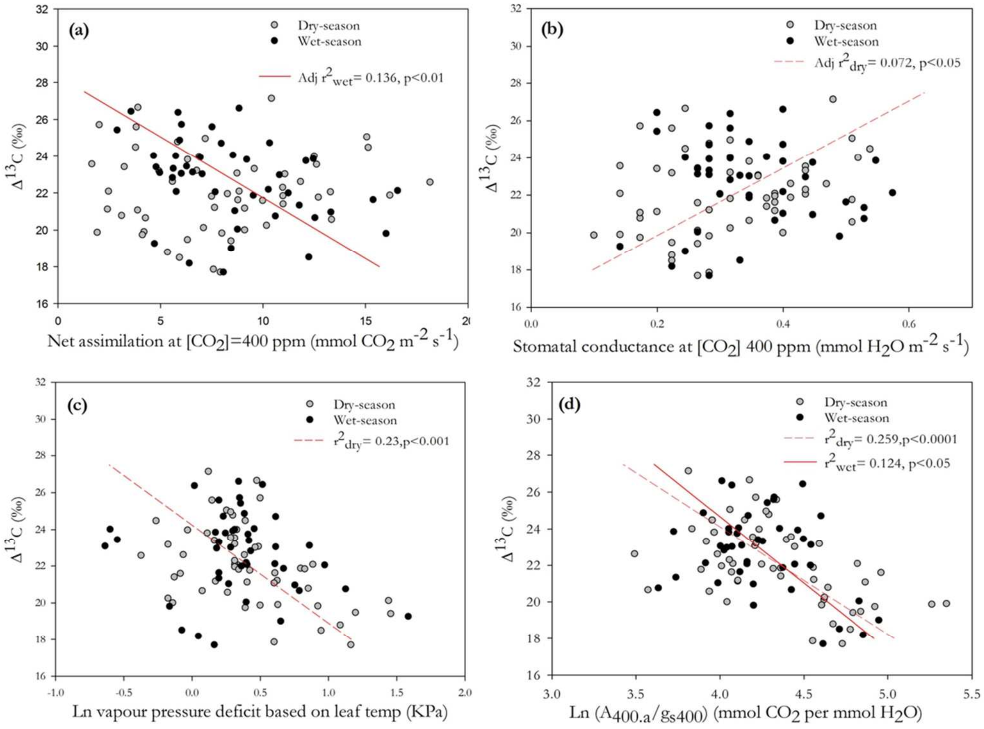

130x100mm (300 x 300 DPI)

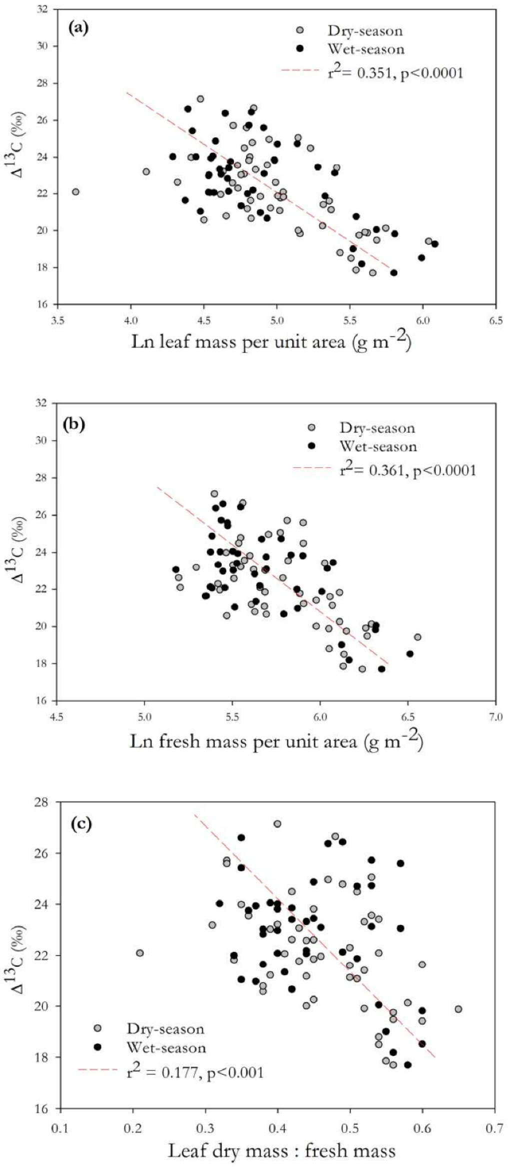

413x951mm (300 x 300 DPI)

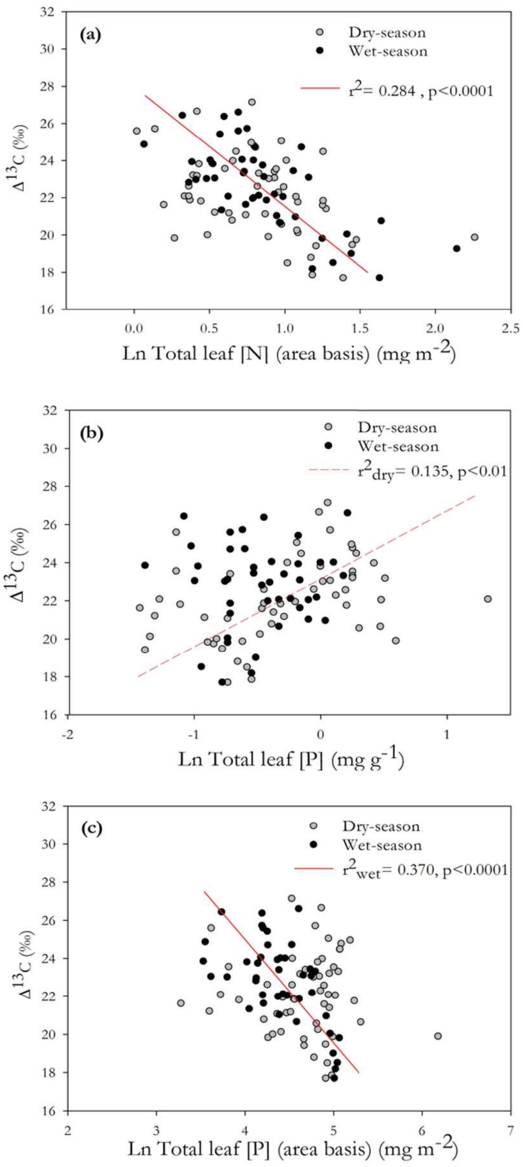

254x566mm (300 x 300 DPI)